UPPSALA
UNIVERSITET

# The Magnetocaloric Effect in Antiferromagnetic and Noncollinear Magnets

Siri A. Berge

Master's degree project in Material Science
30 credits, 1FA690

Supervisor:
Anders Bergman

Subject reader:
Heike Herper

Examinator:
Biplab Sanyal

June 14, 2023

# Abstract

The magnetocaloric effect (MCE) is the temperature change in a magnetic material due to a change in an applied magnetic field. How the MCE behaves in different magnetic materials and at different phase transitions is fundamental to understand. The driver of the MCE is a change in entropy which has multiple contributions: magnetic, lattice, and electron. In this thesis the MCE is studied in a simple antiferromagnetic (AFM) model and in a realistic noncollinear spin glass Neodymium model using Monte Carlo and Atomistic Spin Dynamics simulations. For the simple AFM system, no clear results were achieved, indicating that MCE in AFM materials is not due to a change solely in the magnetic entropy. For the complex magnetic material Nd, a more clear result is seen, indicating that frustration in the system might be important to the MCE in noncollinear materials. Nd results also signify more phase transitions than previously reported.

# Populärvetenskaplig sammanfattning

Magnetiska kylskåp är kanske framtidens kylskåp. De drivs av ett magnetiskt fenomen som förekommer i vissa material. När sådana material sätts under ett varierande magnetfält ändras deras temperatur, vilket kan nyttjas i bland annat kylskåp. Fenomenet kallas den magnetokaloriska effekten.

Den magnetokaloriska effekten förekommer i magnetiska material och beroende på materialets egenskaper har den olika styrkor vid olika temperatur. Varför magnetiska kylskåp inte ännu är en vardagsapparat är just för att det inte har upptäckts ett material som har en stark nog effekt att driva ett kylskåp vid rumstemperatur men effekten används redan idag för kylning i special sammanhang, till exempel i viss vetenskaplig utrustning, ofta vid väldigt låga temperaturer.

Det finns dock många olika magnetiska material, varav en klass av dem kallas ickekolinjära. Kolinjära magnetiska material är de som är mest studerade, till dessa tillhör, till exempel, en vanlig kylskåpsmagnet, som har en permanent magnetism och som är ferromagnetisk. Detta betyder att alla små magnetiska moment som vi kan approximera sitter på varje atom, i till exempel järn, pekar åt samma håll. Antiferromangetism är också kolinjärt men vartannat magnetiskt moment pekar åt motsatta håll vilket ger noll nettomagnetism totalt. Ickekolinjär magnetism innebär att relationen mellan alla små atomiska magnetiska moment är lite mer komplicerad än så. Till dessa material inkluderas neodym som ofta används som en tillsats i starka permanenta magneter blandat med elementen järn och bor men som själv inte har en nettomagnetism.

I min uppsats har jag studerat den magnetokaloriska effekten i neodym som är ett väldigt komplext magnetism system samt i en simpel antiferromagnet med hjälp av datorsimuleringar av de individuella magnetiska momenten i materialet.

I den antiferromagnetiska modellen såg jag ingen tydlig magnetokalorisk effekt, vilket indikerar att endast ett magnetiskt bidrag inte ger en stor respons. Detta innebär att mer studier bör genomföras för att undersöka hur magnetostrukturella förändringar påverkar responsen då denna studie endast inkluderade magnetiska förändringar och inte strukturella. Sedan i neodym såg jag att det kanske finns fler fasövergångar än tidigare trott i materialet, vilket också skulle behöva en närmare studie. Det finns också en tydligare magnetokalorisk respons i neodym än i den antiferromagnetiska modellen, vilket indikerar att magnetisk frustration gör skillnad för effektens beteende.

# Contents

# 1 Introduction

The climate crisis is a pressing issue on the world and there is a necessity for more energy efficient devices. Cooling and refrigeration systems account for an approximated 17% of electricity consumption world wide [1]. The current most common method for refrigeration is vapor-compression technology, which while safe and reliable, has adverse environmental impacts due to the refrigerants, which accounts for an approximated 7.8% of global greenhouse gas emissions [2]. Magnetic refrigeration has been proposed as a way to improve upon this inefficiency [3, 4].

Magnetic refrigeration technology was first proposed in the early 20th century as independent discoveries by Debye in 1926 [5] and Giauque in 1927 [6] when both showed cooling of paramagnetic salts during adiabatic demagnetization. The next important steps towards magnetic refrigeration occurred in the late 20th century; in 1976, a first proof-of-principle of a near room temperature magnetic refrigerator was built [7] and following that, a boom of prototype magnetic refrigerators [8–10]. The next large discovery was the giant magnetocaloric effect in 1997 which opened up the field further for room-temperature refrigeration [11, 12]. However, the technology is not yet commonplace.

The magnetocaloric effect (MCE) is the change in thermal state a material undergoes under a varying applied magnetic field. This is what magnetic refrigeration technology is based on. The giant magnetocaloric effect occurs when the temperature change is large compared to most other magnetocaloric materials, making it more efficient in refrigeration. The effect occurs due to rearrangement of the atomic magnetic moments in the magnetocaloric material when a magnetic field is applied, changing the entropy of the system. Entropy is a measure of the disorder in a system and is described through thermodynamics. The entropy has several contributions from the different ways the system can be disordered: the magnetic, the lattice and the electronic. When the entropy decreases in the material due to an applied field, it is called the conventional MCE; if the entropy increases, it is called the inverse or unconventional MCE. Materials have different ground state spin arrangements described by the interactions between them, for example most permanent magnets are ferromagnetic (FM), where all spins are aligned, resulting in a net magnetic moment in the material. The MCE behaves differently for each arrangement and studying the MCE behavior depending on the magnetic state of a material is important for a more complete understanding of the MCE.

There are many interesting magnetic materials with different magnetic grounds states and phases; ferromagnetism is just the tip of the iceberg. Antiferromagnetism occurs when every atomic spin moment is aligned antiparallel to its neighbor creating a magnetic structure with spontaneous magnetization but no net magnetic moment. Magnetic states where the spins are not aligned parallel or antiparallel are called noncollinear, and can be quite complicated. Neodymium has been recently shown to be a spin glass, a type of noncollinear system, which exhibits aging and has no long range order [13] making it an excellent candidate to study MCE in complex magnetic systems.

Since the MCE is due partially to spin interactions in a material, atomistic spin dynamics and Monte Carlo methods can be used to study it. Atomistic spin dynamics (ASD) is the simplification of treating a spin localized at each atom position and calculating the dynamics of the spins due to their interactions using an equation of motion. Monte Carlo methods are used to understand the energy landscape of a material using stochastic algorithms. One code package which can be used for these types of simulations is UppASD [14] developed at Uppsala University, which is used in this study.

The purpose of this thesis is to study the magnetocaloric effect in antiferromagnetic and noncollinear magnetic materials using atomistic spin dynamics and Monte Carlo methods with UppASD.

# 2 Theory

## 2.1 Magnetism

Magnetism comes in all shapes and sizes. It exists due to the quantum mechanical spin inherent in particles, of which electrons have relatively strong magnetic moments. In each atom, depending on the electron configuration, the electrons might contribute to a total magnetic moment for the atom, which would make the material magnetic. Electrons exist in a spin up or down state and there are quantum mechanical rules described by Hund's rules for their possible states in the atomic electron shells. Filled shells have paired electrons and so have equal number of up and down spins, negating the total magnetic moment. If a shell is partially filled, there will be unpaired electrons contributing to a total magnetic moment of the atom resulting in a magnetic material. Iron, the most well known magnetic material, has six electrons in its outer shell, resulting in four unpaired electrons due to Hund's rules which contribute to the total magnetic moment of each iron atom.

The most simple magnetic states are collinear, meaning the atomic spins lie in the same or opposite direction. This includes permanent magnets such as ferromagnets (FM) and ferrimagnets as well as magnetic materials which exhibit antiferromagnetism (AFM), see Figure 1. The above named magnetic configurations all occur at temperatures below a critical temperature, $T_{Curie}$ for ferromagnetism and $T_{Néel}$ for antiferro- and ferrimagnetism. Above this temperature, the systems become paramagnetic (PM), where there is zero net magnetic moment and the atomic spins are disordered.

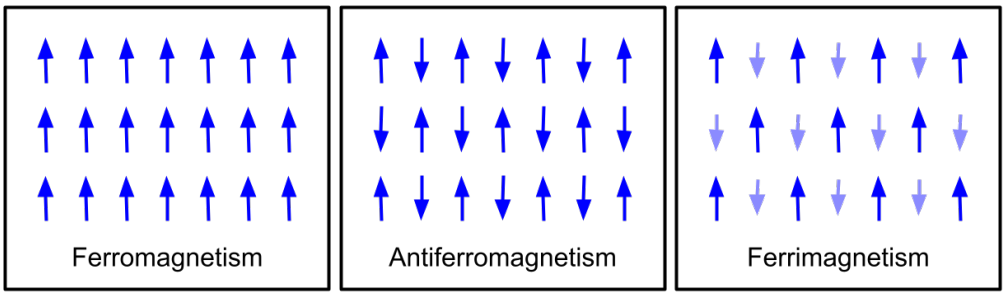


Figure 1: Three common types of collinear magnetism, where all spins lie in the same or opposite direction. Antiferromagnetic systems have zero net magnetic moment while ferromagnetic and ferrimagnetic systems have a non-zero net magnetic moment.

Magnetic frustration occurs when all local interactions cannot be fulfilled simultaneously, meaning that the energy of each interaction cannot be simultaneously minimized [15]. A simple example of this is an antiferromagnetic interaction on a triangular lattice; the spins at two atomic sites of the triangle have opposite orientation but the third does not have a clear orientation since it cannot be the opposite of both of the other spins at the same time, see Figure 2. In this example there are six possible energy equivalent states, called low-energy excitations, which the system can fluctuate between. The incompatibility of the spin-spin interactions and the symmetry of the lattice leads to this magnetically frustrated magnet. These types of systems are noncollinear since the magnetic spin structure is not aligned parallel or antiparallel to each other.

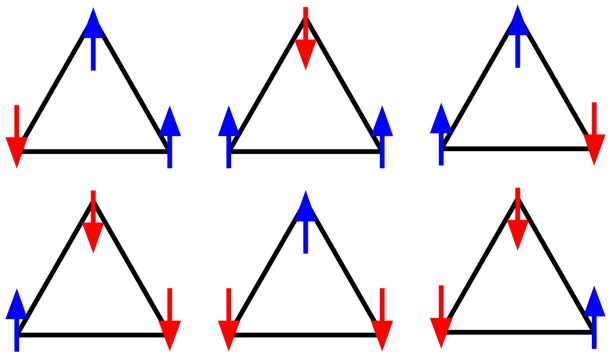

Figure 2: The six lowest energy configurations of system with antiferromagnetic interactions on a triangular lattice.

### 2.1.1 Spin Glass and Neodymium

A spin glass is an interesting magnetic state which exhibits frustrated magnetism and other interesting properties. It is characterized by magnetic disorder, with random types of interactions such that spins are randomly aligned and lack long-range order, not unlike the amorphous lattice of glass, hence the name [16]. The disorder of the interactions, both ferromagnetic and antiferromagnetic, result in frustration of the lattice. Spin glasses also display aging, where the magnetic state depends on the history of the system and time. They are meta stable so compared to a ferromagnet, for example, which has one clear energy minima, the energy landscape of a spin glass has multiple minima, some separated by a small barrier and some by a large barrier.

Neodymium has recently been shown to have a self-induced spin glass state as its elemental crystalline ground state [13, 17]. The element is well-known in the context of magnetism, due to the strong permanent magnets made of an alloy of Nd-Fe-B, colloquially known as 'neodymium magnets'. However, until recently the magnetic ground state of the pure element was still under debate. That the spin glass state of Nd is classified as self-induced is due to that the spin-spin interactions are not random and the spin moments are ordered in spin spirals with varying wavelengths. In conventional spin glass, there is no measure of order. It is also unique that it is a single element rather than an alloy of different elements with a low amount of magnetic atoms which all other discovered spin glasses have been. Neodymium has a double hexagonal close-packed structure (dhcp) presented in Figure 3b alongside a body centered cubic (bcc) structure present in iron.

It has been published that Nd has two phase transitions, one from the spin glass state to a magnetic phase of spin spirals with no glassiness then to the paramagnetic phase [17]. This result is reproduced from the original paper in Figure 9.

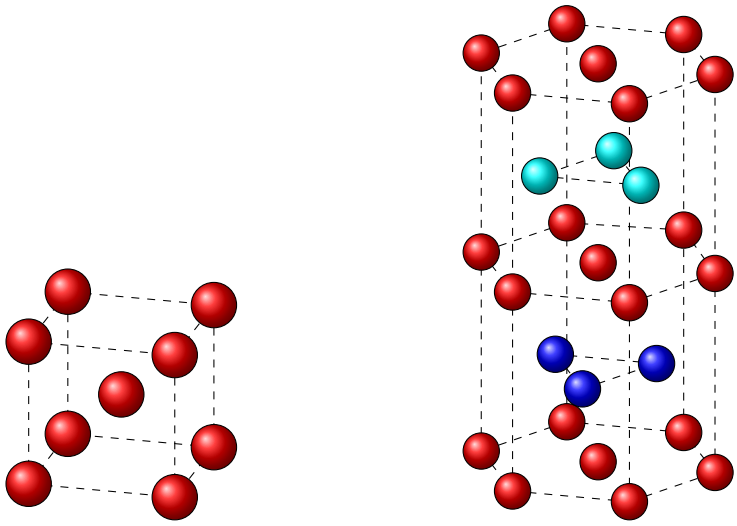

(a) A bcc structure. (b) A dhcp structure.

Figure 3: Body-centered cubic (bcc) structure found in iron and double hexagonal close-packed (dhcp) structure found in neodymium.

### 2.1.2 Heisenberg Hamiltonian

To describe the energy of a magnetic system a model Hamiltonian is necessary. The most common one for magnetic systems is called the Heisenberg model given as

$$H = -\frac{1}{2}\sum_{i \neq j} J_{ij}\mathbf{m}_i \cdot \mathbf{m}_j \tag{1}$$

where $\mathbf{m}_i$ is the magnetic moment at atomic site $i$ and $J_{ij}$ the interatomic exchange parameter which describes how the energy changes due to the rotation of the spins. A positive $J_{ij}$ is a ferromagnetic interaction and a negative an antiferromagnetic interaction. The exchange parameter often depends on distance between the atomic spins and often the parameter decreases with spin-spin separation distance. The model can then be set up such that the exchange parameter is approximated to zero after some specified distance. For example a nearest neighbor model can be used where all $J_{ij}$ but the ones where $i$ and $j$ are nearest neighbor are set to zero. However, to make the model more realistic and also for cases where the lattice structure is more complicated, $J_{ij}$ terms are included for several more neighbors at increasing interatomic distances. These terms can be calculated using density functional theory and the LKAG method [18–20].

The coupling between the spins is due to multiple sources depending on the material type. There is direct coupling, where the wavefunctions overlap and interact according to the Pauli principle [21]. There is is also indirect coupling, where it is mediated by a secondary particle, such as itinerant conduction electrons, which is called the Rudermann-Kittel-Kasuya-Yosida (RKKY) interaction [22–24]. This interaction is oscillatory and decreases with distance, however it is also gives rise to relatively long-range coupling in comparison to direct coupling. Since it is oscillatory it includes both FM and AFM interactions depending on distance.

An external magnetic field interacting with the atomic spin moments can also be included in the model through an additional term, the Zeeman term:

$$\mathcal{H} = -\frac{1}{2}\sum_{i \neq j} J_{ij}\mathbf{m}_i \cdot \mathbf{m}_j + \mathbf{H}\sum_i \mathbf{m}_i \tag{2}$$

where $\mathbf{H}$ is an external magnetic field.

### 2.1.3 Atomistic Spin Dynamics

As mentioned previously, each atomic spin is viewed as a magnetic moment at each site and to understand the dynamic behavior of the atomic spins, an equation of motion is necessary. The precession of a magnetic moment due to a torque from a magnetic field is described by

$$\frac{\mathrm{d}\mathbf{m}_i}{\mathrm{d}t} = -\gamma \mathbf{m}_i \times \mathbf{B}_i \tag{3}$$

where $B_i$ is the effective field experienced by the atomic moment at each lattice point $i$ and $\gamma$ the gyromagnetic ratio. The effective magnetic field is given by

$$\mathbf{B}_i = -\frac{\partial \mathcal{H}}{\partial \mathbf{m}_i} \tag{4}$$

where $\mathcal{H}$ is a sum of relevant energy terms such as the Heisenberg exchange interaction and the Zeeman energy, see Equation 2.The effective field is thus, partly, the induced field from the collective atomic moments in the system.

Since the precession is not infinite realistically, a damping term must be included. In the field of micromagnetics, the damping term of choice is often the Gilbert damping torque. Replacing the right-hand side of the cross product in Equation 3 with the effective field $\mathbf{B}_i$ plus the damping term produces the Landau-Lifshitz-Gilbert (LLG) equation

$$\frac{\mathrm{d}\mathbf{m}_i}{\mathrm{d}t} = -\gamma \mathbf{m}_i \times \mathbf{B}_i + \frac{\alpha}{m_i}\mathbf{m}_i \times \frac{\partial \mathbf{m}_i}{\partial t} \tag{5}$$

which can be rewritten in the form of the original Landau-Lifshitz equation

$$\frac{\mathrm{d}\mathbf{m}_i}{\mathrm{d}t} = -\gamma_L \mathbf{m}_i \times \mathbf{B}_i - \gamma_L \frac{\alpha}{m_i}\mathbf{m}_i \times (\mathbf{m}_i \times \mathbf{B}_i) \tag{6}$$

using a scalar Gilbert damping constant $\alpha$ assuming isotropic damping and the renormalized gyromagnetic ratio $\gamma_L$, which is defined as

$$\gamma_L = \frac{\gamma}{(1+\alpha)^2}. \tag{7}$$

The above equations are only valid at 0K. To include finite temperature effects in the equation of motion another torque is considered from the thermal fluctuations in the system. This is a stochastic torque and is included as a noise term through an additional field $\mathbf{B}_i^{fl}$ in the stochastic Landau-Lifshitz-Gilbert (SLLG) equation

$$\frac{\mathrm{d}\mathbf{m}_i}{\mathrm{d}t} = -\gamma_L \mathbf{m}_i \times (\mathbf{B}_i + \mathbf{B}_i^{fl}) - \gamma_L \frac{\alpha}{m_i}\mathbf{m}_i \times [\mathbf{m}_i \times (\mathbf{B}_i + \mathbf{B}_i^{fl})] \tag{8}$$

which describes the motion of atomic moments. At each site $i$ in the lattice, the magnetic moment $\mathbf{m}_i$ experiences an effective magnetic field $\mathbf{B}_i$ and a stochastic magnetic field $\mathbf{B}_i^{fl}$. In the equation, the first term is the processional motion and the second the damping motion. Finite temperature effects are included through the fluctuation field in the SLLG equation since the size of the field is associated with the temperature of the atomistic spins. For more details see [20].

## 2.2 The Magnetocaloric Effect

The Magnetocaloric Effect (MCE) is the change in thermal state a material undergoes under a varying applied magnetic field. It was first discovered by Weiss and Piccard in 1917 during experiments to map magnetization as a function of field and temperature in nickel [25, 26].

### 2.2.1 Thermodynamics

The magnetocaloric effect is discussed in terms of thermodynamics and often measured in the change in entropy of the material or the adiabatic temperature change. The laws of thermodynamics include the zeroth law, that two systems in equilibrium with a third are in equilibrium with each other. The first law states that energy is conserved. The second law states that the total entropy of interacting systems never decrease. The third and last law states that a system approaching absolute zero approaches zero entropy.

To begin with, the internal energy $U$ of a system can be described by a function of entropy $S$, volume $V$, and magnetic field $H$ or magnetic moment $M$ [27]:

$$U = (S,V,M) = (S,V,H) \tag{9}$$

such that

$$dU = TdS + HdM. \tag{10}$$

The system may also be described by the temperature $T$, volume $V$, pressure $P$, and entropy, such that

$$dU = TdS - PdV \tag{11}$$

from which the heat capacity can be defined as

$$C_V = \frac{\partial U(T,H)}{\partial T} \tag{12}$$

for a system of constant volume while letting the internal energy depend on temperature and external field as in Equation 10.

The entropy is given by

$$S(T,H) = S_0 + \int_0^T \frac{1}{T'} \frac{\partial U(T',H)}{\partial T} dT' = S_0 + \int_0^T \frac{C_v(T',H)}{T'} dT' \tag{13}$$

where $S_0$ is an integration constant and can be set to zero since entropy should vanish at absolute zero according to the fourth postulate of thermodynamics.

The entropy can also be computed from the magnetization M in the system as

$$\Delta S(T, 0 \to H) = \int_{H_0}^{H_1} \left( \frac{\partial M}{\partial T} \right)_H dH. \tag{14}$$

which is often useful in experimental settings. The quantity which is used to study the magnetocaloric effect is the change in entropy which is usually defined as the difference in entropy between a system with no field and a system with some finite field given by H. This is written as

$$\Delta S(T, 0 \to H) = \Delta S(H_1 \to H_2) = S(T, H_2) - S(T, H_1 = 0). \tag{15}$$

However, often the temperature difference is also included when discussing MCE, which is given by

$$\Delta T(T, 0 \to H) = -\int_0^H \frac{T}{C_{H'}} \left( \frac{\partial M}{\partial T} \right)_{H'} dH'. \tag{16}$$

The entropy for a magnetic system can be written as [28]

$$S(T,H) = S_M(T,H) + S_e(T,H) + S_l(T,H) \tag{17}$$

where $S_M$ is the magnetic entropy, $S_e$ the electron contribution and $S_l$ the lattice contribution to the entropy assuming no electron-phonon interaction. Often it is thought that only the magnetic contribution will have a field-induced change which is non-negligible. This picture of the entropy contributions is however a just a useful simplification. In reality these contributions are not decoupled from each other and this simplification may even be a hindrance when discussing some phenomena, for example in cases of magnetostructural phase transitions.

### 2.2.2 MCE Scheme

When a magnetic field is applied to a conventional magnetocaloric material, the material will increase in temperature, and the material will return to its original temperature when the magnetic field is removed. However, if there is a heat sink, the material will cool down to a temperature below the initial temperature when the magnetic field is removed. This magnetic refrigeration scheme is shown schematically in Figure 4.

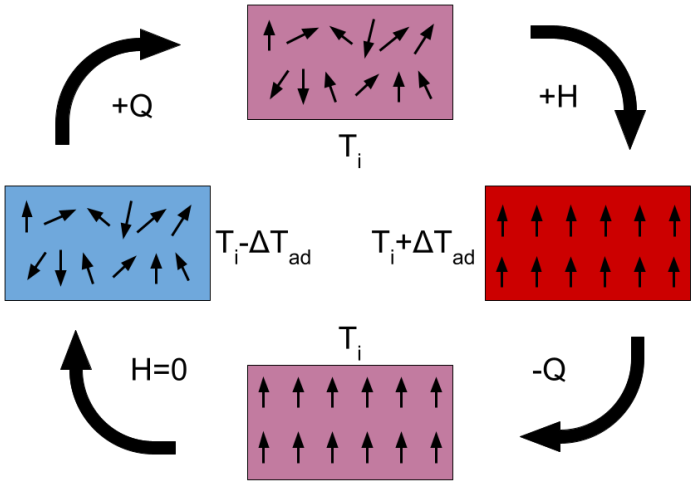


Figure 4: Magnetic refrigeration scheme using the conventional magnetocaloric effect in a ferromagnetic material where Q is some heat quantity and $\Delta T_{ad}$ is the adiabatic temperature variation.

The effect is the result of an entropy change. When a magnetic field is applied isothermally to a magnetic material with some finite temperature, the atomic spins will rotate to account for the field. This will result in a decrease of the entropy of the system in the case where there is a decrease of the disorder of the arrangement of spins. This is an isothermal process marked with a red arrow from state $a$ to state $b$ in Figure 5. Following this, there is an adiabatic process, marked with a blue arrow from state $b$ to state $c$, which is the removal of the field. This process results in a temperature change from $T_i$ to $T_f$, whose difference is $\Delta T_{ad}$. Since the magnetic field is removed adiabatically, the entropy is conserved. However, the arrangement of spins returns to a disordered state when no magnetic field is applied, leaving the only free variable, the temperature, to decrease to accommodate the conservation of the entropy. The temperature decrease, physically is due to a decrease in the vibrational energy in the lattice to accommodate for the

conservation of entropy and the third law of thermodynamics.

To note, is that generally the largest change in entropy occurs over a magnetic phase transition, for example a ferromagnetic to paramagnetic phase transition since there is a large change in the order of the spin structure. Transition temperatures in some materials may also be field dependent to allow for even greater manipulation of the MCE. Some materials have several phase transitions and so there can exist several temperatures in the material at which a large MCE can be obtained. The type of phase transition might also be relevant to the size of the effect, such as an order-to-order or an order-to-disorder transition.

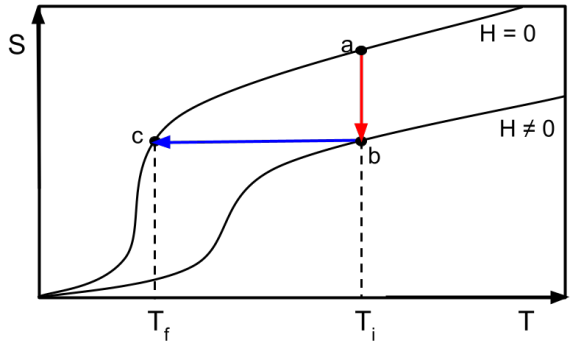


Figure 5: Qualitative Entropy versus Temperature for the refrigeration process of conventional MCE where the red arrow from a to b indicates an isothermal process at temperature $T_i$ and the blue arrow from b to c indicates an adiabatic process from $T_i$ to $T_f$.

In the case of unconventional MCE, the entropy increases with the addition of an external magnetic field, since an applied field increases the disorder of the spin configuration [29]. With the same thermodynamic processes as presented in Figure 5, the cycle would result in a net increase of the temperature of the system. Often there is a misconception that AFM materials exhibit inverse MCE, however this is not true. While some antiferromagnetic materials have been discovered to be unconventional magnetic materials at certain temperatures [30], however many antiferromagnetic materials exhibit both conventional and unconventional MCE in different temperature intervals [31–33] and some show only conventional MCE [34–36].

### 2.2.3 Magnetic Refrigeration

Magnetic refrigeration, on the other hand, was realized separately from the magnetocaloric effect by Debye in 1926 [5] and Giaque in 1927 [6] who, independently of each other, conducted experiments of the adiabatic demagnetization of paramagnetic salts resulting in low temperatures. The first magnetic refrigerator proof-of-concept for near-room temperature was built as early as 1976 by G. V. Brown [7]. Previous to this seminal paper, magnetic refrigeration was primarily concerned with cooling at temperatures below 20K [37]. When the Giant-MCE was discovered in an alloy of Gd-Si-Ge in 1997 by Pecharsky and Gschneidner [11], the discussion of potential real-world applications began. The main challenges in building a magnetic refrigerator is in producing the magnetic field and heat transfer [38].

Unconventional magnetocaloric materials have been proposed to be used in conjunction with conventional as the heat sink necessary for the isothermal application of magnetic field in the refrigeration process [30, 39, 40].

### 2.2.4 Magnetocaloric Materials

When looking at magnetocaloric materials and their potential applicability in refrigeration, two values are most important, the change in entropy and at which temperature this occurs. This partly determines how effective the material is and at which temperatures it can be utilized in. Other properties are also relevant, such as hysteresis, however in general these two values are looked at first. For applications, generally materials with transitions in the cryogenic temperature range and room-temperature are of interest, for specialized applications of the former and common-use of the latter.

Some magnetocaloric materials are presented in Table 1 alongside relevant values and phase transition types for comparison. Elemental gadolinium and the famous Giant-MCE gadolinium alloy $Gd_5Si_2Ge_2$ are presented with both fields 2T and 5T to give an impression of the increase in $-\Delta S$ due to field strength.

Of note is the material $Mn_5Si_3$, which has both inverse and conventional MCE at different transitions including a noncollinear AFM phase, two AFM phases, and finally a PM phase [33]. The material has been studied in several iterations, theoretically and experimentally [45] including the similar material $Mn_{5-x}Fe_xSi_3$ [46] and it has been claimed that spin-fluctuations drive the inverse magnetocaloric effect in this material [47].

Table 1: Some magnetocaloric materials presented with relevant values for comparison and type of phase transition (NC AFM = noncollinear AFM and MP = some magnetic phase) with transition temperature $T_c$ [K]. The change in entropy is negative, so a negative value is the inverse MCE.

| Material | Phase transition | $T_c$ [K] | -$\Delta$S [J/kgK] | $\Delta$T [K] | $\Delta$H [T] | Ref. |
|---|---|---|---|---|---|---|
| $Gd_5Si_2Ge_2$ | FM - PM | 277 | 14 | 7.5 | 2 | [41] |
| $Gd_5Si_2Ge_2$ | FM - PM | 277 | 19 | 15 | 5 | [41] |
| Gd | FM - PM | 294 | 5.5 | 5 | 2 | [42] |
| Gd | FM - PM | 294 | 11 | 13 | 5 | [42] |
| MnAs | FM - PM | 318 | 32 | 13 | 5 | [43] |
| $Ni_{50}Mn_{37}Si_{13}$ | FM - FM | 299 | -18 | 12 | 5 | [30] |
| $ErRu_2Si_2$ | AFM - FM | 5.5 | 17.6 | 12.9 | 5 | [34] |
| $Mn_5Si_3$ | NC AFM - MP | 45 | -2.5 | - | 5 | [33] |
| $Mn_5Si_3$ | MP - AFM | 55 | 2 | - | 5 | [33] |
| DySb | FM - PM | 11 | 16 | - | 5 | [44] |
| $La_{0.125}Ca_{0.875}MnO_3$ | AFM - PM | 125 | -3 | - | 5 | [31] |
| $ErNi_{0.6}Cu_{0.4}Al$ | AFM - FM | 9 | 22.5 | - | 5 | [35] |

In the literature of antiferromagnetic MCE materials, several report a magnetostructural phase transition rather than a solely magnetic transition, for example in $Mn_{0.8}Fe_{0.2}Ni_{1-x}Cu_xGe$ with $x = 0.05$-$0.3$ [32]. DySb is also an interesting material with a field-induced phase transition AFM to FM which is described to be the reason behind an inverse MCE at low field strengths and low temperatures [44], but presented here is the values at 5T in field strength.

$ErRu_2Si_2$ is also an interesting material since at a AFM to FM phase transition a Giant-MCE effect is seen comparable to the gadolinium based alloys, though at a cryogenic temperature.

## 2.3 Monte Carlo Methods

Monte Carlo methods can also be used to study the energy landscape of magnetic systems. Instead of solving problems analytically, stochastic methods are used involving randomized numbers to probe the phase space [48]. While many methods exist, the Metropolis-Hastings algorithm [49] is the most common Monte Carlo method and exemplifies how they work.

The algorithm works on the principle of minimizing the energy of the system configuration by making small changes to a reference state $s$ then employing a temperature dependent probability for the system to transition

into the new state $s'$ given by

$$W(s \to s') = \begin{cases} e^{-\beta \Delta E} & if \Delta E > 0 \\ 1 & \text{otherwise} \end{cases} \tag{18}$$

with $\beta = 1/\mathrm{k}_B\mathrm{T}$ for the classical Boltzmann distribution case. The energy is calculated from the Hamiltonian in Equation 2. This results in a finite probability of probing every possible state of the system.

The algorithm follows these steps:

1. Initialize by choosing lattice spin configuration $s$ and calculate the energy.
2. Randomly change the orientation of the spin at a random lattice site, creating state $s'$.
3. Calculate the energy difference between $s$ and $s'$.
4. Generate a random number r, if r $<$ W then $s'$ is the new reference state, otherwise keep previous state $s$.
5. Repeat steps 2-4 until desired convergence is met.

# 3 Method

The simulations were performed using the Uppsala Atomistic Spin Dynamics (UppASD) code package [14] which executes both the Monte Carlo and the atomistic spin dynamics parts of the calculations. The system is first thermalized using a Monte Carlo method then evolved via the stochastic Landau-Lifshitz-Gilbert (SLLG) Equation which is an equation of motion for micromagnetic systems [20, 50]. The code was run on the Tetralith cluster, part of the National Supercomputing Center at Linköping University.

Three systems were studied, one simple bcc-Fe system with the standard FM coupling, an AFM model based on the bcc-Fe system, as well as dhcp-Nd.

In the case of bcc-Fe and the unrealistic AFM model, the exchange parameters were taken from [51] which includes up to 4th neighbor terms with sign changes made in the AFM case. The size was 40x40x40 bcc unit cells with periodic boundary conditions. AFM is realized through making the bcc structure into two sublattices, where the corner atoms in the unit cell interact ferromagnetically and the corner to center atoms interact antiferromagnetically. This is called a c-type AFM configuration where all the atomic spins in each vertical column point in the same direction, but the next nearest column all point in the opposite direction. All interactions used are shown in Figure 6. This is a simple AFM system, with little to no magnetic frustration. The external magnetic field was perpendicular to the aligned spins, with the spins in the x-direction and the field in the z-direction.

For zero H-field, the spin moments were aligned according to the moment file, in the FM case they are aligned FM and in the AFM case they are aligned AFM. For all other magnetic field strengths, the restart file generated from the zero-field case was used to initialize the system. The systems were thermalized using a heat bath method, which is a Monte Carlo method, then statistics were taken during a spin dynamics simulation, which has been outlined previously in this report. The time step was 0.1 femtoseconds and the damping parameter was 0.5. From this the internal energy of the system can be found for each desired temperature and external field, from which the heat capacity and entropy are found according to Equation 12 and 13 respectively.

In the case of dhcp-Nd, the exchange couplings were taken from [13]. The size was 96x96x10 with periodic boundary conditions. The system was first annealed with a heat bath Monte Carlo method, then atomistic spin dynamics were run to take statistics. The time step was 1 femtosecond with damping 0.5. The spin configuration in the system was initialized with

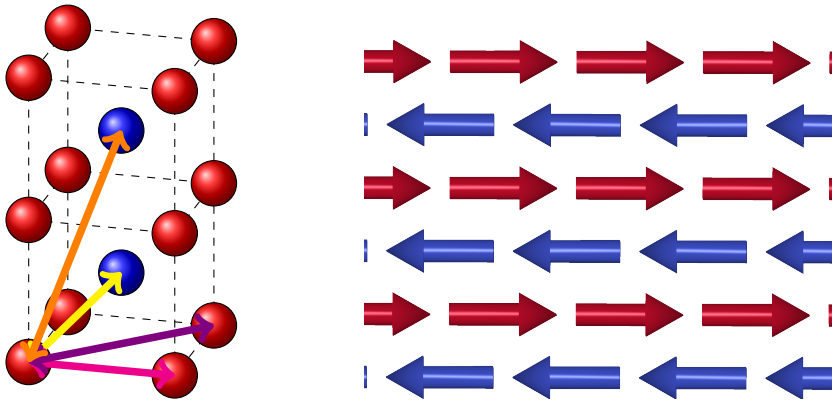

(a) (b)

Figure 6: (a) Exchange interactions are shown as arrows. First (yellow arrow) and fourth (orange) neighbor are AFM and second (magenta pink) and third (dark purple) are FM. Blue filled balls show moments that are aligned, as for red filled balls, but there is an antiferromagnetic interaction between red and blue filled balls. (b) AFM system at 0K from simulation.

specified moments from a restart file. The field is set along the z-direction.

Since this method only allows changes in the magnetic structure in the systems while the lattice remains fixed, only the magnetic contribution to the entropy is studied.

# 4 Results

Simulations were run for three systems: realistic FM bcc-Fe used as a benchmark for comparison, an unrealistic AFM model based on the bcc-Fe system and realistic dhcp-Nd. The heat capacity and change in entropy is shown for all systems, while the energy and entropy are only presented for the Fe system.

## 4.1 FM bcc-Fe

The results of ferromagnetic iron are presented in Figure 7. Iron shows the expected behavior of a peak at 900K due to a magnetic phase transition from FM to PM. The Curie temperature, is experimentally given as 1040K, however the lower value of the temperature here is a result of retrieving the exchange parameters from density functional theory and the discrepancy is expected. In the entropy, Figure 7c, the shift between curves of 0-2 T and 3-5 T is due to different discretization of the temperature in the different simulations. The heat capacity reaches a maximum of approximately 420 J/kgK compared to the experimental specific heat capacity 440 J/kgK. These results reproduces previous studies.

The heat capacity, Figure 7b, shows a clear peak at 900K with small differences in the maximum value depending on the magnetic field strength, with the maximum for 0T and minimum peak height for 5T. The change in entropy is presented in Figure 7d. A clear peak is seen at 900K for field strengths 1T to 5T. For larger magnetic field, the maximum of -$\Delta S$ increases, starting at 1 J/kgK for 1 T field up to 3 J/kgK for 5 T field. In comparison to the values of Table 1, these are relatively small values for $-\Delta$S. With external fields below 1 T, there is no clear peak, which suggests that this is noise in the range of $\Delta \mathrm{S}_M \approx \mp 0.5$ J/kgK indicating the precision in this simulation.

## 4.2 Simple AFM model

The results of the simple AFM model are presented in Figure 8. The heat capacity, Figure 8a shows a single clear peak at the phase transition temperature of the Fe system and is also very similar in shape and magnitude to the heat capacity curves of the Fe system, presented in Figure 7b. For the AFM system, the change in the maximum of the heat capacity peak depending on the field strength is not seen as clearly as previously.

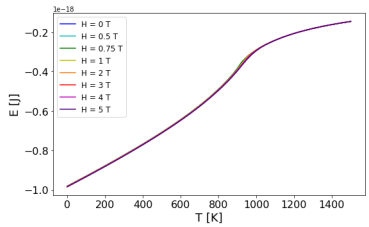


(a) E

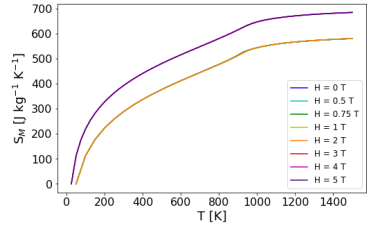


(b) $S$

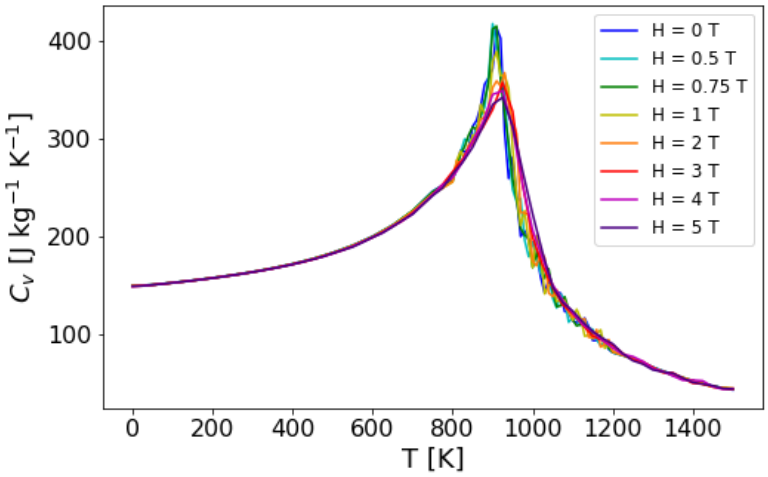


(c) $C_v$

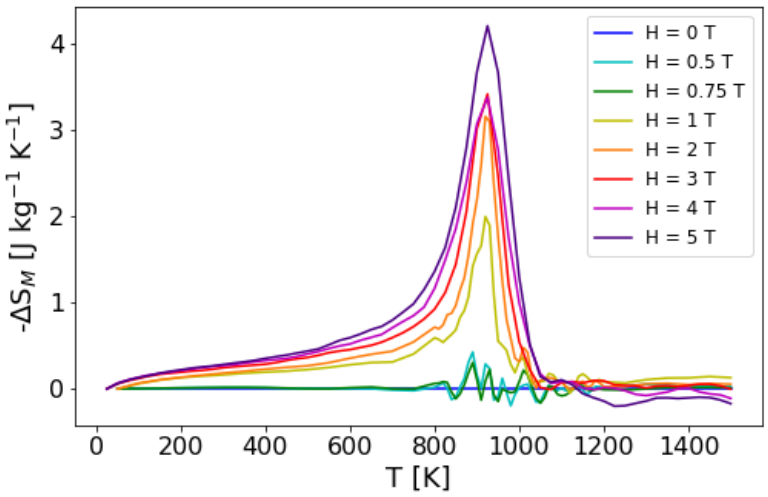


(d) $\Delta S_M$

Figure 7: Results of ferromagnetic bcc Fe. (a) Energy curve and (b) entropy curve. (c) The heat capacity show a clear peak indicating the magnetic phase transition at 900K. (d) Clear peak at the magnetic phase transition for field strengths above 1T.

As for the change in entropy, Figure 8b, there are no clear peaks or trends in the curves and the values are a magnitude smaller than those for the FM ground state. Since the curves are within $\Delta S_M \approx \mp 0.5$ J/kgK, which is most likely not within the precision of the simulation of the Fe system, and these two simulations are exactly the same with exception of the signs of the exchange parameters, the conclusion might be drawn that this is also not within the simulation precision. This is despite the large field strengths used. It is clear that something occurs at the magnetic phase transition, however, in cannot be resolved through this data.

## 4.3 dhcp-Nd

In the Nd system, there are multiple peaks in the heat capacity, Figure 10a, implying several phase transitions in the temperature interval 0K to 16K. Previously published results reproduced in Figure 9, show two phase transitions, one at 4K and another at 11.5K. The first is the transition from a self-induced spin glass state to a spin spiral state and the second the transition from a spin spiral state to a paramagnetic state. These two are reproduced by the results of this thesis, however more structure is seen close to the 4K peak. At 5K a clear peak is seen whose magnitude is the same for all magnetic field strengths. There is another structure at around 4.5K, however this is not as well resolved compared to the other three peaks since there are differences in the magnitude of the curves of the different field strengths. In the published results, the peak at 4K is wide and has some shape present at a slightly higher temperature, around 5K, indicating the additional peak structure seen in this report. All in all, another phase might be present between the self-induced spin glass phase and the spin spiral phase in elemental Nd.

The change in entropy in the Nd system presents two structures that stand out, one at 5K and another at 11.5K. The peak at 11.5K is seen in the heat capacity and reflects the paramagnetic phase transition. The consistency of the shape of the curves at 11.5K show that there is a clear magnetocaloric response, albeit small, with a maximum of approximately $\Delta S_M$ = -0.1 J/kgK. This is much smaller than what was previously noted as outside of the precision of the simulation, but since this is a widely different simulation than the bcc-Fe and AFM simulations, the absolute values and precision are not comparable in the same way as between the two previous models. Dissimilar to the bcc-Fe peak, for which the magnitude of the peak increased with the field strength, the Nd results do not. This is perhaps because the interaction strength in Nd is much lower and the magnetic field

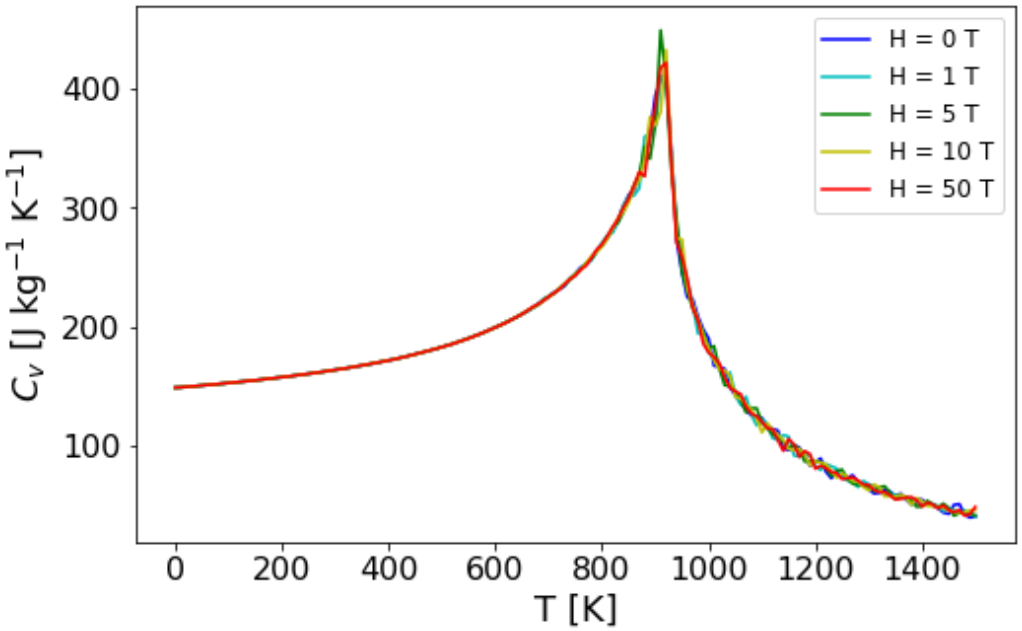


(a) $C_v$

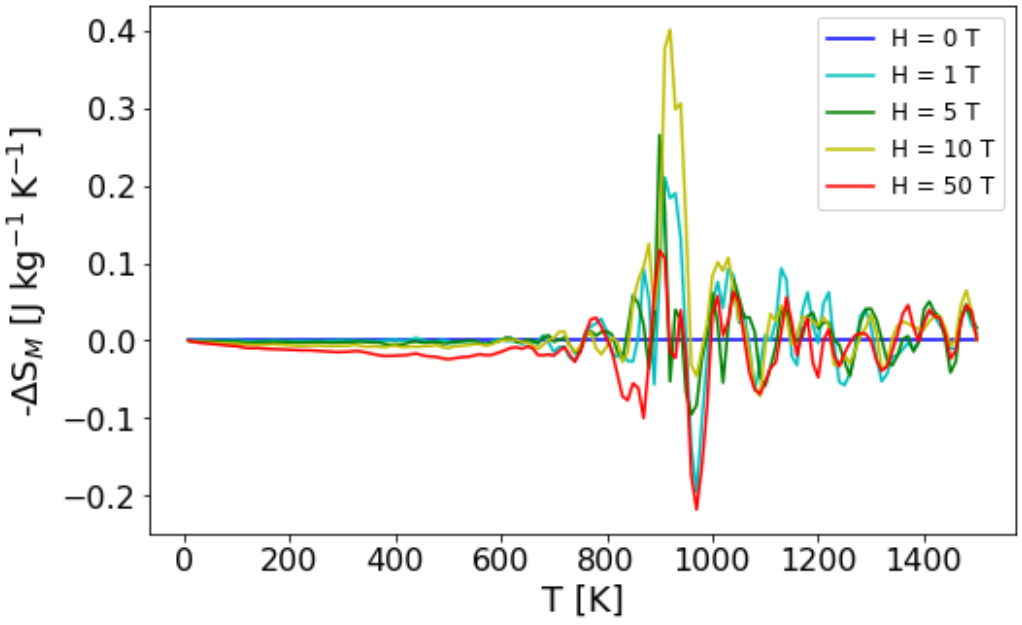


(b) $\Delta S_M$

Figure 8: (a) Heat capacity and (b) change in entropy of c-type AFM in bcc Fe with magnetic fields from 0 T to 50 T. There is one phase transition at 900K.

strengths used are comparatively large.

The structure present at around 5K in the change in entropy is not as clear with no common trend like the paramagnetic transition peak since only two of the curves, 0.5T and 6T, make up the negative peak while the rest have positive peaks. In the results this discrepancy is most likely due to that the simulation is not fully resolved around this temperature as seen in the heat capacity. It might also be noted that it is reasonable that at around this temperature the system undergoes a transition from the self-induced spin glass state to a spin spiral state, which would most likely have an inverse MCE response since this transition goes from a more disordered state to a less disordered state. This could mean that the two negative curves indicate this, however no solid conclusion can be drawn regarding this based purely on these results. There is also a lack of a peak at 4K where one might be expected due to the transition which is clearly seen in both the published results and in this report.

All of the heat capacity curves presented have similar shapes for each peak. For example, the shape of the $C_v$ peak at 11.5K in Nd and the heat capacity curves for both Fe models, start relatively flat, to then reach the peak quickly, then have a drop to about the same magnitude as prior to the peak, to finally drop off at a slower rate.

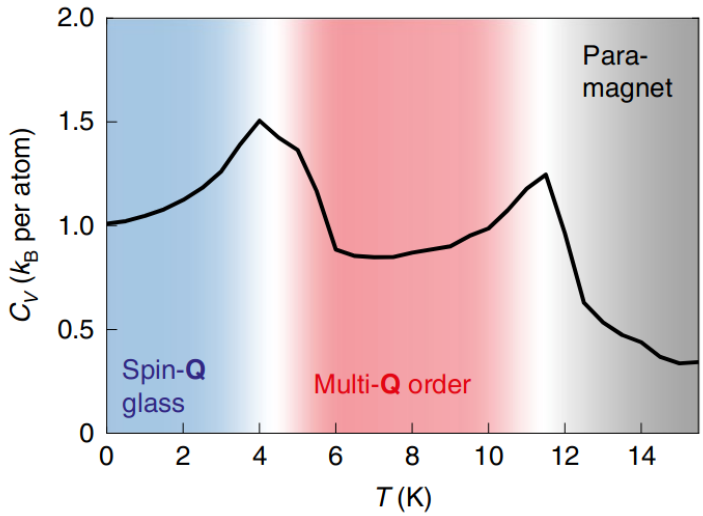


Figure 9: Heat capacity in elemental Nd reported in Verlhac, B. et al. (2022) [17] fair use permitted by CC4.0.

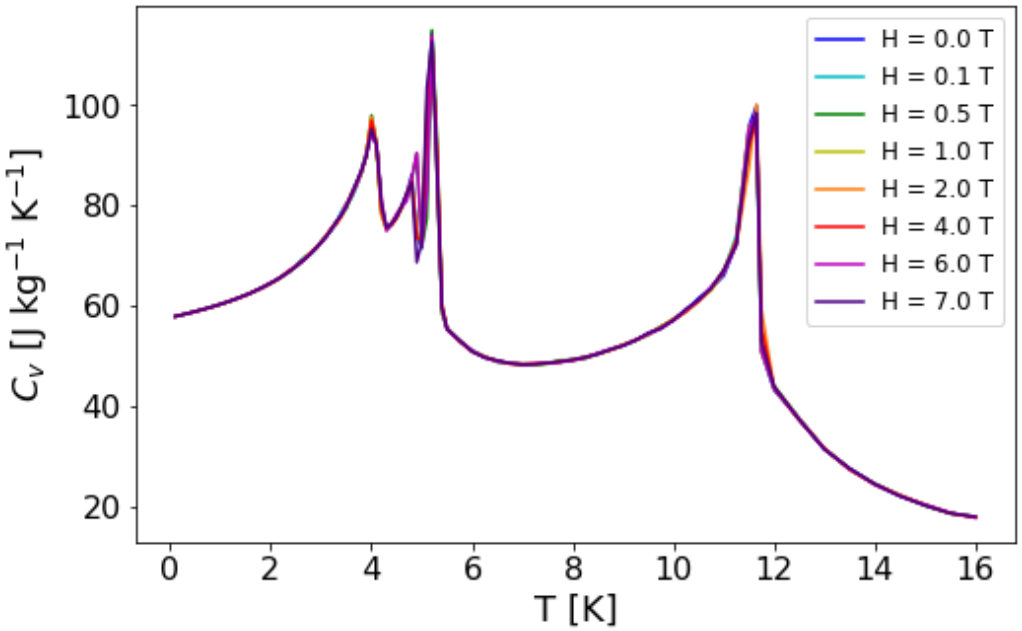


(a) $C_v$

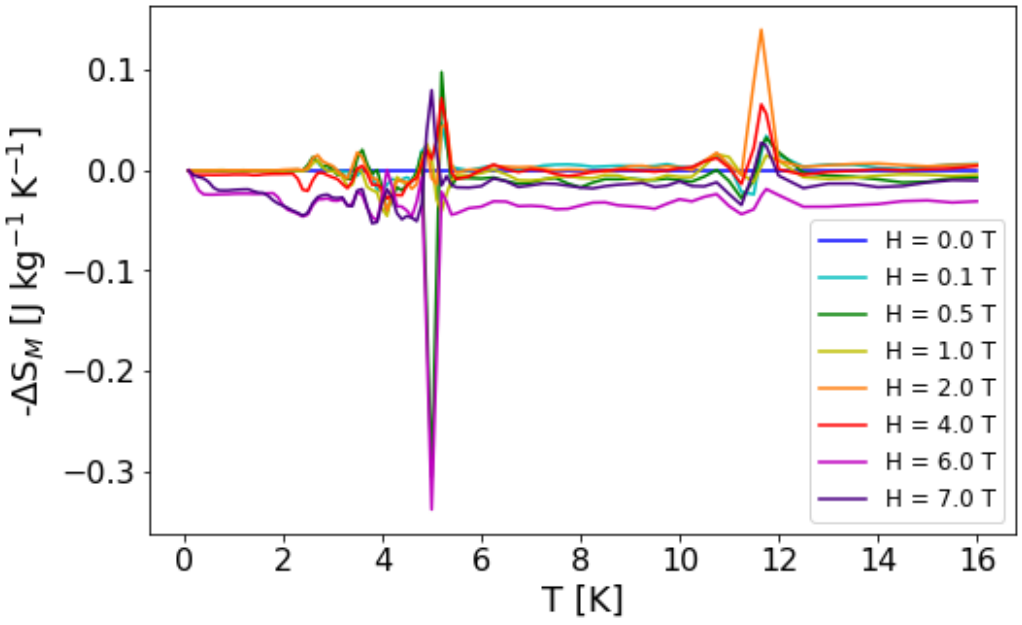


(b) $\Delta S_M$

Figure 10: Simulation results of dhcp-Nd. The heat capacity (a) shows four peaks at 4K, 4.5K, 5K, and 11.5K. The change in entropy (b) reflects two of the peaks, those at 5K and 11.5K.

# 5 Discussion

AFM materials are not necessarily expected to have large MCE responses since they have no net magnetic moment and given how AFM spin configurations interact with magnetic fields. In the case of a simple AFM system, such as the one studied here, the magnetic order is quite stable meaning the magnetic frustration is minimal. If a magnetic field is oriented along the aligned atomistic spin direction, no large changes would be expected, however, if they are aligned perpendicular to each other then some disorder might arise from a large enough field. Despite this, it is clear from experimental studies that there are large MCE responses in AFM materials such as $ErRu_2Si_3$ [30] presented in Table 1. Fe is known for having low magnetic anisotropy and Nd is thought to be isotropic such that the field direction should not make a large difference due to this factor.

There is a large limitation in assuming that only the magnetic contribution to the entropy is non-negligible which was assumed earlier when discussing the contributions to the entropy given in Equation 17. It has been shown that the lattice contribution to the entropy is as large as the magnetic contribution in hcp-Gd [52] and that for a full understanding of the entropy of a system not only the magnetic contribution can be studied. Structural changes have not been included in this study, which could have a large impact on the MCE results, since often it is unclear whether the lattice transition forces a magnetic transition or vice versa, a so called magnetostructural transition. Since the method used here only allows for changes in the magnetic configurations and not lattice changes, the only entropy contribution that is calculated is the magnetic part. This report cannot say anything about the lattice contribution to the entropy. With this in mind, the results of the AFM system can be considered.

The change in the magnetic entropy of the FM and AFM systems look similar when the external field is below 1 T in the FM system. Since the curves within 0.5 J/kgK might be considered noise in the FM system, the parallel can be drawn that all curves in the AFM system are noise, despite the large magnetic fields applied, 10 T and 50 T. This would imply that there is no sole magnetic contribution to the entropy and that this term might even be negligible in the total sum in Equation 17 for AFM systems. Any magnetic contribution is then most probably driven by a magnetostructural transition in this case as seen clearly in some materials listed in the section on MCE materials.

In the case of bcc-Fe, the interactions are very long range, and since only a few exchange parameters are used, this simulation set-up might not be enough to capture the the MCE response for smaller field strengths, such as 0.75T, as seen in Figure 7d. This should also be considered for the AFM model system since the same Fe parameters except sign are used. However, if more exchange parameters are included, the system would become more frustrated and not be as simple a model as was wanted in this project. Further, a more realistic AFM version of an Fe system would also probably be smaller in volume and the heat capacity peak should appear at a lower temperature value than is seen in this report, but for this to be examined density functional theory calculations would be necessary.

The neodymium results show several things. In the heat capacity, there are indications of more phase transitions than previously reported. The additional structure around 4.5K and 5K is very prominent in the simulation, however what kind of phases this might be due to is unclear and not within the scope of this work. Further studies of the phases of Nd are necessary to determine if there are additional phases and what they might be. In terms of the MCE response in Nd, a clear, but small peak is seen at the paramagnetic phase transition, but the response is unresolved in the temperature region 4K to 5K. Here it might be expected to see inverse MCE due to the reported phase transition from the self-induced spin glass state to a non-collinear spin spiral state, however no conclusion can be drawn about this from these results.

A point of comparison between the AFM system and the Nd system, is the level of magnetic frustration present. These were both studied to be able to compare them, since one is simple and one very complex. The made-up AFM material studied was of c-type AFM in a bcc structure. This has very small frustration in it, compared to the Nd system which describes a spin glass with spin spirals which has a much larger level of frustration. Since a response is seen in the Nd results, albeit small, it should be considered whether the amount of magnetic frustration in the system contributes to a larger MCE response. This would be a much larger study, starting from ab initio density functional theory, to make a large scale study of MCE in magnetically frustrated systems including the separate entropy contributions.

In the context of the applicability of these materials for magnetic refrigeration, there is no great use for them. Compared to the giant MCE materials based on gadolinium or manganese, some presented in Table 1, the change in entropy is very small in the studied materials. For neodymium particularly, only a small response was seen at a low temperature and a large response

would not have been expected. The greater motivation for this study is that it is interesting to understand the MCE in unusual magnetic materials.

The difficulty of making successful simulations should not be understated. A balance must be found between computational time and the size and number of steps of the simulation in order to also produce results which can be interpreted from a physics perspective. Changing the initial spin configuration or the number of exchange parameters also has a great impact. In the case of the simple AFM model, where no clear simulation results were found, a decision eventually had to be made whether yet another different simulation would yield a new result or not, since there are endless combinations of input parameters.

## 5.1 Conclusion and outlook

The response of the magnetocaloric effect in an antiferromagnetic system and a model of Nd were studied using Monte Carlo methods and atomistic spin dynamics. The AFM system showed no clear response, especially in comparison to the FM system, indicating that the response is smaller than the precision afforded in the simulation. This could signify that in AFM systems a field-induced magnetostructural transition is what drives the MCE. The Nd system gave a small response but a clear one, compared to the AFM system, from which it might be considered that a more magnetically frustrated material might produce a larger MCE.

This thesis asks more questions than it answers. For future work, it might be interesting to make a large study of how frustration in an AFM system might change the MCE, for example by taking the simple AFM model used here, finding the lattice parameters and exchange parameters from density functional theory and in Monte Carlo simulations increase the number of exchange parameters to increase the frustration. It would also be important to understand further the contributions to the entropy, specifically to study the MCE at magnetostructural phase transitions.

The long history of the question of the magnetic phases of elemental Nd seems to not yet be resolved as indicated by at least one unknown phase in this work. Atomistic Spin Dynamics could be used to study this element in the future to continue to understand its magnetic phases and spin structure, first by working to resolve the unknown peak at 4.5K and to look at the spin structure in the simulation at these temperature values.

# Acknowledgements

Tack till min handledare Anders Bergman som varit lärare och mentor till mig i hela fem år. Tack till Heike Herper för trevlig feedback som ämnesgranskare. Tack till Erik Karpelin för tikz hjälpen. Tack till Anton Gregefalk, Maria Olavarría och Damjan Dagbjartsson för två fina år på mastersprogrammet. Tack till min kära familj.

# 6 Bibliography


[1] Coulomb D, Dupont J. L, Pichard A, and IIF-IIR. The Role of Refrigeration in the Global Economy (2015), 29th Informatory Note on Refrigeration Technologies. Technical report, International Institute of Refrigeration, Paris, France, 2015. Publisher: IIF-IIR.

[2] Morlet V, Coulomb D, Dupont J. L, and IIF-IIR. The impact of the refrigeration sector on climate change, 35th Informatory Note on refrigeration technologies. Technical Report, International Institute of Refrigeration, Paris, France, 2017. Publisher: IIF-IIR.

[3] Andrej Kitanovski. Energy Applications of Magnetocaloric Materials. *Advanced Energy Materials*, 10(10):1903741, 2020. _eprint: https://onlinelibrary.wiley.com/doi/pdf/10.1002/aenm.201903741.

[4] Julia Lyubina. Magnetocaloric materials for energy efficient cooling. *Journal of Physics D: Applied Physics*, 50(5):053002, January 2017. Publisher: IOP Publishing.

[5] P. Debye. Einige Bemerkungen zur Magnetisierung bei tiefer Temperatur. *Annalen der Physik*, 386(25):1154–1160, 1926. _eprint: https://onlinelibrary.wiley.com/doi/pdf/10.1002/andp.19263862517.

[6] W. F. Giauque. A Thermodynamic Treatment of Certain Magnetic Effects. A Proposed Method of Producing Temperatures Consederably Below 1° Absolute. *J. Am. Chem. Soc. 1927, 49, 8, 1864–1870*, 1927. Publisher: American Chemical Society.

[7] G. V. Brown. Magnetic heat pumping near room temperature. *Journal of Applied Physics*, 47(8):3673–3680, August 1976. Publisher: American Institute of Physics.

[8] C. Zimm, A. Jastrab, A. Sternberg, V. Pecharsky, K. Gschneidner, M. Osborne, and I. Anderson. Description and Performance of a Near-Room Temperature Magnetic Refrigerator. In Peter Kittel, editor, *Advances in Cryogenic Engineering*, Advances in Cryogenic Engineering, pages 1759–1766. Springer US, Boston, MA, 1998.

[9] W. A. Steyert. Stirling-cycle rotating magnetic refrigerators and heat engines for use near room temperature. *Journal of Applied Physics*, 49(3):1216–1226, August 2008.

[10] Bingfeng Yu, Min Liu, Peter W. Egolf, and Andrej Kitanovski. A review of magnetic refrigerator and heat pump prototypes built before the year 2010. *International Journal of Refrigeration*, 33(6):1029–1060, September 2010.

[11] V. K. Pecharsky and Jr. Gschneidner, K. A. Giant Magnetocaloric Effect in Gd5(Si2Ge2). *Physical Review Letters*, 78(23):4494–4497, June 1997. Publisher: American Physical Society.

[12] V. K. Pecharsky and K. A. Gschneidner. Effect of alloying on the giant magnetocaloric effect of Gd5(Si2Ge2). *Journal of Magnetism and Magnetic Materials*, 167(3):L179–L184, March 1997.

[13] Umut Kamber, Anders Bergman, Andreas Eich, Diana Iuşan, Manuel Steinbrecher, Nadine Hauptmann, Lars Nordström, Mikhail I. Katsnelson, Daniel Wegner, Olle Eriksson, and Alexander A. Khajetoorians. Self-induced spin glass state in elemental and crystalline neodymium. *Science*, 368(6494):eaay6757, May 2020. Publisher: American Association for the Advancement of Science.

[14] UppASD. https://github.com/UppASD.

[15] A. P. Ramirez. Chapter 4 Geometrical frustration. In *Handbook of Magnetic Materials*, volume 13, pages 423–520. Elsevier, January 2001.

[16] An Introduction to Spin Glasses: History, Simulations and Phase Transition. In Marco Baity Jesi, editor, *Spin Glasses: Criticality and Energy Landscapes*, Springer Theses, pages 3–42. Springer International Publishing, Cham, 2016.

[17] Benjamin Verlhac, Lorena Niggli, Anders Bergman, Umut Kamber, Andrey Bagrov, Diana Iuşan, Lars Nordström, Mikhail I. Katsnelson, Daniel Wegner, Olle Eriksson, and Alexander A. Khajetoorians. Thermally induced magnetic order from glassiness in elemental neodymium. *Nature Physics*, 18(8):905–911, August 2022. Publisher: Nature Publishing Group.

[18] A. I. Liechtenstein, M. I. Katsnelson, V. P. Antropov, and V. A. Gubanov. Local spin density functional approach to the theory of exchange interactions in ferromagnetic metals and alloys. *Journal of Magnetism and Magnetic Materials*, 67(1):65–74, May 1987.

[19] J. Kubler, K.-H. Hock, J. Sticht, and A. R. Williams. Density functional theory of non-collinear magnetism. *Journal of Physics F: Metal Physics*, 18(3):469, March 1988.

[20] Olle Eriksson, Anders Bergman, Lars Bergqvist, and Johan Hellsvik. *Atomistic spin dynamics: foundations and applications*. Oxford University Press, 2017.

[21] Piers Coleman. *Introduction to Many-Body Physics*. Cambridge University Press, 1 edition, November 2015.

[22] M. A. Ruderman and C. Kittel. Indirect Exchange Coupling of Nuclear Magnetic Moments by Conduction Electrons. *Physical Review*, 96(1):99–102, October 1954. Publisher: American Physical Society.

[23] T. Kasuya. A Theory of Metallic Ferro- and Antiferromagnetism on Zener's Model. *Progress of Theoretical Physics*, 16:45–57, July 1956.

[24] Kei Yosida. Magnetic Properties of Cu-Mn Alloys. *Physical Review*, 106(5):893–898, June 1957. Publisher: American Physical Society.

[25] Pierre Weiss and Auguste Piccard. Le phénomène magnétocalorique. *Journal de Physique Théorique et Appliquée*, 7(1):103–109, 1917. Publisher: Société Française de Physique.

[26] Anders Smith. Who discovered the magnetocaloric effect? *The European Physical Journal H*, 38(4):507–517, September 2013.

[27] A. M. Tishin and Y. I. Spichkin. *The magnetocaloric effect and its applications*. Series in condensed matter physics. Institute of Physics Pub., Bristol, 2003.

[28] A. M. Tishin. Magnetocaloric effect in strong magnetic fields. *Cryogenics*, 30(2):127–136, February 1990.

[29] P. J. von Ranke, N. A. de Oliveira, B. P. Alho, E. J. R. Plaza, V. S. R. de Sousa, L. Caron, and M. S. Reis. Understanding the inverse magnetocaloric effect in antiferro- and ferrimagnetic arrangements. *Journal of Physics: Condensed Matter*, 21(5):056004, January 2009.

[30] Thorsten Krenke, Eyüp Duman, Mehmet Acet, Eberhard F. Wassermann, Xavier Moya, Lluis Mañosa, and Antoni Planes. Inverse magnetocaloric effect in ferromagnetic Ni–Mn–Sn alloys. *Nature Materials*, 4(6):450–454, June 2005. Publisher: Nature Publishing Group.

[31] Anis Biswas, Sayan Chandra, Tapas Samanta, M. H. Phan, I. Das, and H. Srikanth. The universal behavior of inverse magnetocaloric effect in antiferromagnetic materials. *Journal of Applied Physics*, 113(17):17A902, May 2013. Publisher: American Institute of Physics.

[32] YaNing Xiao, Hu Zhang, YingLi Zhang, KeWen Long, ChengFen Xing, YuWei Liu, and Yi Long. Large inverse magnetocaloric effect induced by antiferromagnetically magnetostructural transition in Mn0.8Fe0.2Ni1-xCuxGe compounds. *Journal of Alloys and Compounds*, 769:916–921, November 2018.

[33] Roberto F. Luccas, Gabriel Sánchez-Santolino, Alex Correa-Orellana, Federico J. Mompean, Mar García-Hernández, and Hermann Suderow. Magnetic phase diagram, magnetotransport and inverse magnetocaloric effect in the noncollinear antiferromagnet Mn5Si3. *Journal of Magnetism and Magnetic Materials*, 489:165451, November 2019.

[34] Tapas Samanta, I. Das, and S. Banerjee. Giant magnetocaloric effect in antiferromagnetic ErRu2Si2 compound. *Applied Physics Letters*, 91(15):152506, October 2007. Publisher: American Institute of Physics.

[35] L. C. Wang, Q. Y. Dong, Z. Y. Xu, F. X. Hu, J. R. Sun, and B. G. Shen. Low-temperature large magnetocaloric effect in the antiferromagnetic ErNi0.6Cu0.4Al compound. *Journal of Applied Physics*, 113(2):023916, January 2013. Publisher: American Institute of Physics.

[36] Yikun Zhang, Yun Tian, Zhenqian Zhang, Youshun Jia, Bin Zhang, Minqiang Jiang, Jiang Wang, and Zhongming Ren. Magnetic properties and giant cryogenic magnetocaloric effect in B-site ordered antiferromagnetic Gd2MgTiO6 double perovskite oxide. *Acta Materialia*, 226:117669, March 2022.

[37] K. A. Gschneidner and V. K. Pecharsky. Thirty years of near room temperature magnetic cooling: Where we are today and future prospects. *International Journal of Refrigeration*, 31(6):945–961, September 2008.

[38] V. Franco, J. S. Blázquez, and A. Conde. Field dependence of the magnetocaloric effect in materials with a second order phase transition: A master curve for the magnetic entropy change. *Applied Physics Letters*, 89(22):222512, November 2006. Publisher: American Institute of Physics.

[39] R. J. Joenk. Adiabatic Magnetization of Antiferromagnets. *Journal of Applied Physics*, 34(4):1097–1098, April 1963.

[40] Xixiang Zhang, Bei Zhang, Shuyun Yu, Zhuhong Liu, Wenjin Xu, Guodong Liu, Jinglan Chen, Zexian Cao, and Guangheng Wu. Combined giant inverse and normal magnetocaloric effect for room-temperature magnetic cooling. *Physical Review B*, 76(13):132403, October 2007. Publisher: American Physical Society.

[41] A. O. Pecharsky, K. A. Gschneidner, Jr., and V. K. Pecharsky. The giant magnetocaloric effect of optimally prepared Gd5Si2Ge2. *Journal of Applied Physics*, 93(8):4722–4728, March 2003.

[42] S. Yu. Dan'kov, A. M. Tishin, V. K. Pecharsky, and K. A. Gschneidner. Magnetic phase transitions and the magnetothermal properties of gadolinium. *Physical Review B*, 57(6):3478–3490, February 1998. Publisher: American Physical Society.

[43] H. Wada and Y. Tanabe. Giant magnetocaloric effect of MnAs1-xSbx. *Applied Physics Letters*, 79(20):3302–3304, November 2001.

[44] W. J. Hu, J. Du, B. Li, Q. Zhang, and Z. D. Zhang. Giant magnetocaloric effect in the Ising antiferromagnet DySb. *Applied Physics Letters*, 92(19):192505, May 2008. Publisher: American Institute of Physics.

[45] N. Biniskos, F. J. dos Santos, K. Schmalzl, S. Raymond, M. dos Santos Dias, J. Persson, N. Marzari, S. Blügel, S. Lounis, and T. Brückel. Complex magnetic structure and spin waves of the noncollinear antiferromagnet Mn5Si3. *Physical Review B*, 105(10):104404, March 2022. Publisher: American Physical Society.

[46] Songlin, Dagula, O Tegus, E Brück, J. C. P Klaasse, F. R de Boer, and K. H. J Buschow. Magnetic phase transition and magnetocaloric effect in Mn5-xFexSi3. *Journal of Alloys and Compounds*, 334(1):249–252, February 2002.

[47] N. Biniskos, K. Schmalzl, S. Raymond, S. Petit, P. Steffens, J. Persson, and T. Brückel. Spin Fluctuations Drive the Inverse Magnetocaloric Effect in Mn5Si3. *Physical Review Letters*, 120(25):257205, June 2018.

[48] David P. Landau and Kurt Binder. *A Guide to Monte Carlo Simulations in Statistical Physics*. Cambridge University Press, 4th edition, 2014. ISBN: 9780521842389 9780511614460 Publisher: Cambridge University Press.

[49] Nicholas Metropolis, Arianna W. Rosenbluth, Marshall N. Rosenbluth, Augusta H. Teller, and Edward Teller. Equation of State Calculations by Fast Computing Machines. *The Journal of Chemical Physics*, 21(6):1087–1092, June 1953.

[50] B. Skubic, J. Hellsvik, L. Nordström, and O. Eriksson. A method for atomistic spin dynamics simulations: implementation and examples. *Journal of Physics: Condensed Matter*, 20(31):315203, July 2008.

[51] Xiuping Tao, D. P. Landau, T. C. Schulthess, and G. M. Stocks. Spin Waves in Paramagnetic bcc Iron: Spin Dynamics Simulations. *Physical Review Letters*, 95(8):087207, August 2005. Publisher: American Physical Society.

[52] R. Martinho Vieira, O. Eriksson, T. Björkman, A. Bergman, and H. C. Herper. Realistic first-principles calculations of the magnetocaloric effect: applications to hcp Gd. *Materials Research Letters*, 10(3):156–162, March 2022.